
IEEE P802.15
Wireless Personal Area Networks

Project	IEEE P802.15 Working Group for Wireless Personal Area Networks (WPANs)	
Title	Measurement Procedure and Methods on Channel Parameter Extraction	
Date Submitted	20 May, 2004	
Source	[Andreas F. Molisch] [Mitsubishi Electric Research Labs (MERL)] [Cambridge, MA]	Voice: [] Fax: [+1 617 621 7550] E-mail: [Andreas.Molisch@ieee.org]
	[Ulrich G. Schuster] [Swiss Federal Institute of Technology (ETHZ)] [Zurich, Switzerland]	Voice: [+41-44-63-25287] Fax: [+41-44-63-21209] E-mail:[schuster@nari.ee.ethz.ch]
	[Chia-Chin Chong] [Samsung Advanced Institute of Technology (SAIT)] [Suwon, Korea]	Voice: [+82-31-280-6865] Fax: [+82-31-280-9555] E-mail:[chiachin.chong@samsung.com]
Re:	[Response to Call for Contributions on 15.4a Channel Modeling Subgroup.]	
Abstract	[This document describes a unified measurement procedure and methods to extract channel parameters from measurement data.]	
Purpose		
Notice	This document has been prepared to assist the IEEE P802.15. It is offered as a basis for discussion and is not binding on the contributing individual(s) or organization(s). The material in this document is subject to change in form and content after further study. The contributor(s) reserve(s) the right to add, amend or withdraw material contained herein.	
Release	The contributor acknowledges and accepts that this contribution becomes the property of IEEE and may be made publicly available by P802.15.	

Measurement Procedure

by Andy Molisch and Johan Karedal

Multipath profiles are to be measured at various locations, so that the statistics can be determined. We have to distinguish four different scales:

1) Small-scale fading:

In order to determine this, a sufficient number of measurement points has to be taken in an area where large-scale parameters like shadowing are identical. Experience shows that some 50 measurement points per area are a minimum. The measurement point must be spaced $\lambda/2$ or more apart, to allow the measurement points to experience independent fading (though for a small angular spread, this is not guaranteed with this spacing). The different realizations of the channel can be achieved by moving either the TX and/or the RX. Note that if the measurements are done in the 100-900 MHz range, it might be difficult to fit 50 measurement points into a small-scale area when only one of the link ends is moved. It is also important that the statistics within the measurement area are stationary. For example, the situation should not occur where one measurement point has a LOS, while another is shadowed behind an obstacle.

2) Large-scale fading:

Different areas within one building should be measured, that are far enough apart that large-scale propagation processes (including shadowing) are different from area to area. However, the absolute distance between TX and RX should be the same for the different areas.

3) Large-scale areas with different distances between TX and RX should be measured.

4) Variations from building to building should be measured.

The statistics for all of the different scales should be extracted.

When measurements of the angular spectra are also desired, this complicates the situation. The reason for this is the different requirement for the spacing of the (small-scale) measurement points. For the extraction of the small-scale statistics, we want the measurement points as far apart as possible - at a minimum, $\lambda/2$ for the LOWEST involved frequency. For the determination of the angular spectra, we need the measurement points no farther apart than $\lambda/2$ for the HIGHEST involved frequency. The main emphasis of the measurements for the 4a channel model will lie on the small-scale statistics, not on angular spectra.

Parameters that must be determined

- Frequency range
- Number of frequency points
- Number of array elements
- Array element spacing
- Transmit power
- Number of measurement points
- IF bandwidth
- Estimated runtime for one measurement

Equipment to bring

- Network analyser
- Spectrum analyser (to check interference level)
- (At least) 2 HF antenna cables of desired length – with calibration (attenuation) curves
- 2 antennas - with calibration curves
- 2 virtual arrays -with stepper motors
- 2 tripods of the same (achievable) height

Information of the measurement site

- Maps - with lengths, scale and material information
- Pre-determined measurement positions, marked on the map

Small Scale Fading Phenomena in Ultra-Wideband Channels: Channel Sounding and Signal Processing

Ulrich G. Schuster, *Member, IEEE*,

Abstract—The abstract goes here.

I. INTRODUCTION

NO introduction available yet — let's get down to business immediately.

II. LINEAR TIME VARYING SYSTEMS

Modeling Radio channels is a complicated task. The complexity of the solution to Maxwell's equations needs to be reduced to a couple of parameters and some mathematically amenable formulas. The two most important steps towards this goal are the assumption of a linear channel and the description by stochastic methods. Linearity follows from Maxwell's theory as long as the materials are linear. This is a good assumption in general. A stochastic description helps to overcome the complexity of the real propagation environment. The tradeoff here is between the optimal utilization of site-specific propagation features and system robustness. A system designed with full knowledge of the propagation conditions at a certain site would be able to exploit these conditions, resulting in superior performance, whereas a system design based on a stochastic channel model will only achieve average performance — but it will achieve this performance at a wide variety of sites whereas the former will not.

A. The System Functions

The most general description within the framework outlined is thus a stochastic linear time-varying (LTV) system. In a classical paper, Bello [1] derived the canonical representation in terms of system functions. The input-output relation is described by the two-dimensional linear operator \mathbb{H} with kernel $h_0(t, t')$ as¹

$$y(t) = (\mathbb{H}x)(t) = \int h_0(t, t')x(t')dt'. \quad (1)$$

The kernel represents the response of the system at time t to a unit impulse launched at time t' . A more convenient representation for the following derivations can be obtained by changing the time origin²:

$$h(t, \tau) = h_0(t, t - \tau), \quad (2)$$

Ulrich G. Schuster is with the Communication Technology Laboratory, Swiss Federal Institute of Technology (ETH), Zurich, Switzerland. Email: schuster@nari.ee.ethz.ch

¹Unless otherwise indicated, integrals are from $-\infty$ to $+\infty$.

²The following choice of the time origin is just one possibility. For an in depth discussion see the report by Artés et al. [2]

representing the response of the system at time t to a unit impulse launched τ seconds earlier. This representation is commonly referred to as the *time-varying impulse response*. The input-output relation now reads

$$y(t) = \int h(t, \tau)x(t - \tau)d\tau. \quad (3)$$

Equivalent representations can be obtained by Fourier transforms of the time-varying impulse response.

$$L_{\mathbb{H}}(t, f) := \int h(t, \tau)e^{-j2\pi f\tau}d\tau \quad (4)$$

$$S_{\mathbb{H}}(\nu, \tau) := \int h(t, \tau)e^{-j2\pi\nu t}dt \quad (5)$$

$$H_{\mathbb{H}}(\nu, f) := \int h(t, \tau)e^{-j2\pi f\tau}e^{-j2\pi\nu t}dtd\tau \quad (6)$$

where $L_{\mathbb{H}}$ is often referred to as the *time-varying transfer function* or *Weyl Symbol*, $S_{\mathbb{H}}$ is denoted the *(delay-Doppler) spreading function* and $H_{\mathbb{H}}$ the *output Doppler-spread function* or *bi-frequency function* [1], [2]. A graphical representation is shown in Figure 1. There are various interpretations of the

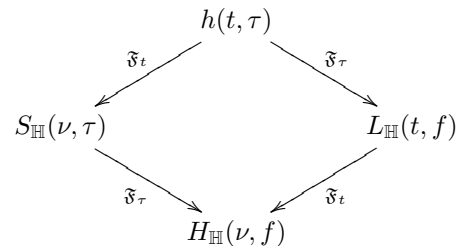


Fig. 1. Relationship between the system functions of an LTV

system functions in terms of a continuum of infinitesimal scatterers giving rise to different delays, Doppler shifts and amplitudes. This physical interpretation is often appropriate for tropospheric scattering channels, but does not necessarily hold for the mobile radio channel.

B. Stochastic Characterization

For a stochastic description, the system functions are modeled as random processes. A complete characterization via associated joint distributions is far too complicated to be of practical interest, hence the description is normally confined to first and second order statistics. If the processes are Gaussian and the channel hence Rayleigh fading, a second order description is indeed a complete statistical characterization. According to the four equivalent system functions, there are

four equivalent correlation functions

$$R_h(t, t', \tau, \tau') := \mathbb{E} [h(t, \tau)h^*(t', \tau')] \quad (7)$$

$$R_S(\nu, \nu', \tau, \tau') := \mathbb{E} [S_{\mathbb{H}}(\nu, \tau)S_{\mathbb{H}}^*(\nu', \tau')] \quad (8)$$

$$R_L(t, t', f, f') := \mathbb{E} [L_{\mathbb{H}}(t, f)L_{\mathbb{H}}^*(t', f')] \quad (9)$$

$$R_H(\nu, \nu', f, f') := \mathbb{E} [H_{\mathbb{H}}(\nu, f)H_{\mathbb{H}}^*(\nu', f')]. \quad (10)$$

These correlation functions depend on four parameters and are still difficult to handle. A further simplification arises if two additional assumptions are introduced: (1) The system is *wide-sense stationary* (WSS) in time and (2) the system is WSS in frequency. The second assumption is also referred to as *uncorrelated scattering* (US), since the fading gains for different delays τ , representing different scatterers, are uncorrelated. Hence the correlation functions simplify

$$R_h(t, t', \tau, \tau') = R_h(t - t', \tau)\delta(\tau - \tau') \quad (11)$$

$$R_S(\nu, \nu', \tau, \tau') = R_S(\nu, \tau)\delta(\nu - \nu')\delta(\tau - \tau') \quad (12)$$

$$R_L(t, t', f, f') = R_L(t - t', f - f') \quad (13)$$

$$R_H(\nu, \nu', f, f') = R_H(\nu, f - f')\delta(\nu - \nu') \quad (14)$$

Because of their importance, some functions are given special names. $C_{\mathbb{H}}(\nu, \tau) := R_S(\nu, \tau)$ is called the *scattering function* of the channel and $R_{\mathbb{H}}(\Delta t, \Delta f) := R_L(t - t', f - f')$ is denoted the *time-frequency correlation function*.

The WSS assumption is generally accepted, at least locally over a reasonable time frame. If shadowing effects come into play, the overall channel is of course no longer WSS. The US assumption however needs to be questioned for UWB channels since it is obvious that channel correlation properties change with frequency. One solution to this problem is to separate the nonstationary behavior from the small scale fading, as for example proposed by Kunisch and Pamp [3]; another possibility is the use of local scattering functions as proposed by Matz [4].

C. UWB Channel Models

The system functions do not depend on the bandwidth and are thus readily applicable to UWB channels. The correlation functions however only contain all statistical information if the channel process is assumed Gaussian. The notion of an infinite continuum of scatterers is approximately satisfied for narrowband channels since many reflections are not resolvable and hence the superposition of many arrivals justifies the invocation of the central limit theorem. In real world UWB channels, the number of scatterers does not necessarily scale linearly with the bandwidth and the Gaussian assumption becomes questionable due to insufficient averaging.

In narrowband channels, a model often used is a tapped delay line expression, where the channel impulse response is described as [5]

$$h(t, t') = \sum_{i=1}^{N(t')} c_i(t)\delta(t' - \tau_i(t))e^{j\theta_i(t)}. \quad (15)$$

$N(\tau)$ is the number of multipath components, $c_i(t)$ the time-varying amplitude, $\tau_i(t)$ the time-varying path delay and $\theta_i(t)$ the time-varying phase. The underlying assumption here is that

each arrival can be associated with a single propagation path, like in a ray-tracing model. This is no longer true for UWB channels since diffraction and dispersion leads to a frequency dependent distortion of every echo. One way to get around this problem is to include linear filters in every path, as in the paper by Qiu [6]. The other possibility is to continue using a tapped delay-line model but dispose of the physical intuition relating distinct paths to channel taps and consider the tapped delay line model just as the standard discretization of a bandlimited random process without ascribe any physical meaning to the individual terms.

III. VNA CHANNEL MEASUREMENTS

Because of the wide bandwidth, UWB channel measurements have been performed predominantly in the frequency domain using a vector network analyzer (VNA) [3], [7]–[11]. Because the sweep time is quite long, the channel has to remain stationary throughout the whole measurement, practically precluding the sounding of time-variant channels. It is thus sufficient to consider a time invariant channel model with impulse response $h(\tau)$ and frequency response $H(f)$. The VNA samples the channel at different frequencies. However, the measurement points returned are not true samples of the channel transfer function.

A. VNA Measurement System response

An idealized VNA transmits a sinusoid for a fixed amount of time according to

$$x(t) = 2g_T(t) \cos 2\pi kFt \quad (16)$$

where g_T is a time-windowing function modeling the limited sample time, F is the frequency step size and k indicates the current measurement point. In the frequency domain, the transmitted signal is thus

$$X(f) = G_T(f - kF) + G_T(f + kF). \quad (17)$$

The channel output as measured at the receiving end is given by

$$V(f) = \left(G_T(f - kF) + G_T(f + kF) \right) H(f). \quad (18)$$

The VNA filters the signal with an RF prefilter of bandwidth $(-B_{RF}/2, B_{RF}/2)$ and baseband equivalent transfer function $G_{RF}(f)$, to obtain

$$Y_{RF}(f) = \left(G_T(f - kF) + G_T(f + kF) \right) \times H(f) \left(G_{RF}(f - kF) + G_{RF}^*(-f - kF) \right). \quad (19)$$

Let

$$H_0(f - kF) = \left(G_T(f - kF)G_{RF}(f - kF) + G_T(f + kF)G_{RF}(f - kF) \right) H(f). \quad (20)$$

Then $Y_{RF}(f)$ can be expressed as $H_0(f - kF) + H_0^*(-f - kF)$. Note that in $H_0(f - kF)$, the first term contains the wanted signal whereas the second term denotes the self-interference due to aliasing of the filters. Depending on the choice of

the time window, this aliasing contribution can normally be neglected. The receiver performs quadrature demodulation³, hence the resulting baseband signal is

$$Y_{BB}(f) = H_0(f) + H_0^*(-f - 2kF) \quad (21)$$

The baseband lowpass filter $G_{BB}(f)$ bandlimits the signal further to $(-B_{BB}/2, B_{BB}/2)$. Assuming that the RF filter and the baseband filter are perfectly bandlimiting and non-overlapping, the remaining terms at twice the carrier frequency are suppressed completely.

$$\begin{aligned} Y(f) &= Y_{BB}(f)G_{BB}(f) \\ &= H(f + kF)G_{RF}(f)G_{BB}(f) \\ &\quad \times \left[G_T(f) + G_T(f + 2kF) \right] \\ &\quad + H(f + kF)G_{RF}^*(-f - 2kF)G_{BB}(f) \\ &\quad \times \left[G_T(f) + G_T(f + 2kF) \right] \\ &= H(f + kF)G_{RF}(f)G_{BB}(f) \\ &\quad \times \left[G_T(f) + G_T(f + 2kF) \right]. \end{aligned} \quad (22)$$

Furthermore, it is reasonable to assume that the RF filter bandwidth is larger than the baseband filter bandwidth and that the RF filter has a flat passband, such that $G_{RF}(f)G_{BB}(f) = G_{BB}(f)$, and hence

$$Y(f) = H(f + kF)G_{BB}(f) \left[G_T(f) + G_T(f + 2kF) \right]. \quad (23)$$

Finally the VNA correlates the baseband signal with the receive window $g_R(t)$, which is time-limited to $(-T_R/2, T_R/2)$, yielding

$$\begin{aligned} Y[k] &= \int y(t)g_R(t)dt \\ &= \int Y(\varphi)G_R(f - \varphi)d\varphi \Big|_{f=0} \\ &= \int Y(\varphi)G_R(-\varphi)d\varphi \\ &= \int H(\varphi + kF)G_{BB}(\varphi) \\ &\quad \times \left[G_T(\varphi) + G_T(\varphi + 2kF) \right] G_R(-\varphi)d\varphi \\ &\approx \int H(\varphi + kF)G_{BB}(\varphi)G_T(\varphi)G_R(-\varphi)d\varphi, \end{aligned} \quad (24)$$

neglecting the self-interference term. The receive and transmit windows are real; if they are furthermore matched such that $g_R(t) = g_t(t)$, then $G_R(-f) = G_T^*(f)$, and (24) simplifies to

$$Y[k] = \int H(\varphi + kF)G_{BB}(\varphi)|G_{R,T}(\varphi)|^2d\varphi. \quad (25)$$

It can be seen that one sample of the VNA actually contains a weighted average of the channel impulse response within a frequency band determined by the baseband filter bandwidth. Note that I removed any amplifier gain and any path loss

³The demodulation step is actually an approximation, since the LO signal at the receiving end is also time-windowed. Assuming infinite sinusoids, as implicitly done here, is for mathematical convenience. This approximation is justified if the baseband time window is completely contained in the window gating the demodulation signal.

in the preceding calculations and normalized the up- and downconversion steps. To take into account not only the small-scale response, the path loss can be reintroduced through a multiplicative constant.

B. VNA Measurement Noise

Using the standard assumption of white Gaussian noise introduced at the receiver front end with power spectral density (PSD) $\mathcal{N}_0/2$, the PSD after the RF filtering stage is

$$\frac{\mathcal{N}_0}{2} |G_{RF}(f - kF) + G_{RF}(-f - kF)|^2, \quad (26)$$

and after demodulation and baseband filtering

$$\begin{aligned} &\frac{\mathcal{N}_0}{2} |G_{RF}(f)|^2 |G_{BB}(f)|^2 \\ &= \frac{\mathcal{N}_0}{2} |G_{BB}(f)|^2, \end{aligned} \quad (27)$$

again assuming that the baseband filter is contained within the flat part of the RF filter transfer function with unit gain. Note that the total amount of noise corrupting the measured signal is reduced if the filter bandwidth is small. The baseband noise process, denoted $n(t)$, is now correlated with the receive window, yielding

$$N[k] = \int n(t)g_R(t)dt. \quad (28)$$

Let the correlation function of $n(t)$ be denoted $R_n(\tau)$, given by the inverse Fourier transform of (27). Then the sampled noise is characterized by the correlation

$$\begin{aligned} \mathbb{E}[N[k]N^*[k']] &= \delta_{k,k'} \iint \mathbb{E}[n(t)n^*(t')]g_R(t)g_R^*(t')dt dt' \\ &= \delta_{k,k'} \iint R_n(t - t')g_R(t)g_R^*(t')dt dt'. \end{aligned} \quad (29)$$

The noise samples are uncorrelated between the different frequency points since the measurements are performed sequentially, assuming enough time between each sample point to let the filters settle again.

IV. CHANNEL TAP DISTRIBUTION

As already mentioned in Section II-C, the central limit theorem does not necessarily hold for UWB channels since there might not be enough unresolvable arrivals. It is thus important to characterize the distribution of the channel taps. The samples measured by the VNA are not ideal, hence any statement about densities and distributions of these VNA samples does not necessarily carry over to the original physical channel. If the channel process can be modeled as Gaussian, then the VNA samples from equation (25) will also be Gaussian. However, since the VNA samples are a smoothed version of the channel frequency response, they might still appear Gaussian due to the inherent averaging, even if the channel frequency response can no longer be described by a Gaussian process. In addition to the averaging effect, the receiver noise is always present, adding another Gaussian component. Hence to get close to the original channel, the baseband bandwidth B_{BB} should be chosen as small as practically possible, and high SNR conditions should always be ensured.

A. Time Domain Channel Tap Distribution

The frequency domain representation and the time domain representations are linked via the discrete Fourier transform (DFT). Because only a finite bandwidth $B = KF$ is measured, the frequency samples are implicitly windowed. To reduce sidelobes due to the rectangular window, further windowing is often performed in practice. Let $W[k]$ denote the window function, then the IDFT is given by

$$\begin{aligned} y[n] &= \frac{1}{K} \sum_{k=0}^{K-1} W[k] Y[k] e^{j2\pi \frac{n}{K} k} \\ &= \frac{1}{K} \sum_{k=0}^{K-1} W[k] e^{j2\pi \frac{n}{K} k} \\ &\quad \times \int H(\varphi + kF) G_{BB}(\varphi) |G_{R,T}(\varphi)|^2 d\varphi \end{aligned} \quad (30)$$

For ease of notation, define $G(f) := G_{BB}(f) |G_{R,T}(f)|^2$ with inverse Fourier transform $g(t)$. Expressing $H(f)$ as the Fourier transform of $h(t)$, (30) reads

$$\begin{aligned} y[n] &= \frac{1}{K} \sum_{k=0}^{K-1} W[k] e^{j2\pi \frac{n}{K} k} \\ &\quad \times \iint h(t) e^{-j2\pi k F t} e^{-j2\pi \varphi t} G(\varphi) dt d\varphi \\ &= \int \frac{1}{K} \sum_{k=0}^{K-1} W[k] e^{j2\pi \frac{n}{K} k} e^{-j2\pi k \frac{B}{K} t} h(t) \\ &\quad \times \int e^{-j2\pi \varphi t} G(\varphi) d\varphi dt. \end{aligned} \quad (31)$$

With the definition

$$w[n, t] := \frac{1}{K} \sum_{k=0}^{K-1} W[k] e^{j2\pi \frac{n}{K} k} e^{-j2\pi k \frac{B}{K} t} \quad (32)$$

the time domain impuls response can finally be expressed as

$$y[n] = \int w[n, t] g(-t) h(t) dt. \quad (33)$$

Hence all of $h(t)$ contributes to a single sample of the channel impulse response, and thus the same comments apply as for the frequency domain case.

B. Testing Distributions

The tap gain distribution commonly refers to the distribution of the tap magnitude. Because the phase undergoes rapid changes whenever the path distance changes by more than a fraction of a wavelength, the standard assumption is a uniform phase distribution. For UWB signals with lower frequency bound over 1 GHz, this assumption still seems to be valid, hence in the following I will focus on the distribution of the $|y[n]|$ only.

The empirical probability density function (PDF) and cumulative distribution function (CDF) of a measured channel tap $|y[n]|$ can be obtained from the histogram, provided that a sufficient number of independent samples is available. Estimating the true distribution however is more a philosophical problem as to be of practical interest, since the concept of

a true distribution drawn from which samples are observed, requires a probability model within which to operate. Hence the notion of a single true distribution is not relevant — the goal is to find a model that is supported by the measured data and at the same time amenable for analytical and simulation use. The goal is then to test a certain number of predefined mathematical models against the data. The choice of candidate PDFs in this case is based on experience and mathematical convenience. The more degrees of freedom a PDF has the better the fit in general, but the higher the complexity. Thus the right way to proceed is not to find the model with the best fit but the model attaining a prescribed goodness of fit with the least complexity. Typical candidate PDFs for mobile radio channels are Rayleigh, Rice, Nakagami, Gamma, Lognormal and to a lesser extend Weibull. This is a hypothesis testing problem with multiple hypothesis. However, all these PDFs have one or more free parameters, so the hypothesis is the statement that the channel tap random variable is drawn from a distribution belonging to the Rayleigh, the Rice, the Nakagami etc. family. A short summary of hypothesis testing and a discussion of goodness-of-fit tests is contained in Appendix II.

Some researchers propose to first estimate the parameters of all candidate PDFs and then perform the simple hypothesis test only for these parametrized PDFs. Yet though intuitively appealing, this method is not well justified for some tests.

1) *The Kolmogorov-Smirnov Test:* A common hypothesis test for distributions is the *Kolmogorov-Smirnov* test for continuous CDFs. It is based on the fact that the test statistic $\sqrt{n}D_n := \sqrt{n} \sup_x |F_n(x) - F(x)|$ has a limiting CDF for $n \rightarrow \infty$ which does not depend on the test CDF F and the empirical CDF F_n , derived from n samples of the process. Now, if a CDF with estimated parameters is used instead of the fixed CDF, this theorem no longer holds and the test result is meaningless [12].

2) χ^2 *Test:* The χ^2 test was originally developed to test a sample against a discrete distribution. The procedure can be extended to continuous distributions and it even works to some extend for distributions where the parameters need to be estimated. Some theory and explanations are summarized in Appendix II. The general procedure is as follows:

- Partition the range of the random variable in intervals C_j . There is no rule how to choose these intervals, but a equidistant partition seems to make sense. Even for distributions with unlimited range, only a limited number r of intervals are needed, since only intervals containing measured data points are necessary.
- Count the number N_j of measurements that lie in each interval j .
- Either estimate the parameters θ of the distribution under test from the unpartitioned or the partitioned data. See Appendix II for elaboration.
- Compute the test statistic according to (61) or (64), depending on the type of parameter estimate.
- compare the statistic to the integral over the right tail of the χ^2_{r-1-k} PDF at confidence level α and with $r - 1 - k$ degrees of freedom, or equivalently the value of the CDF $Q(1 - \alpha)$. Here k is the number of parameters

compute $w[n, t]$ if $W[k]$ is rectangular

consequences for modeling? How to check for the distribution of the continuous time channel?

this is only to check the distribution of the measured channel — what about the underlying continuous time channel?

estimated from the data. Hence the number of degrees of freedom of the distribution is reduced if parameters need to be estimated first. If the test statistic is larger than the probability obtained by evaluating the integral, the hypotheses must be rejected.

C. Kullback-Leibler Information Divergence

where does this one fit in?

D. Least Squares Fit

and this one?

V. PARAMETER ESTIMATION

A. Mean and Variance

B. Nakagami m Parameter

compute from correlation function or use non-parametric estimate?

C. Delay Spread

frequency dependence of delay spread?

VI. ESTIMATING THE CORRELATION FUNCTIONS

A. Correlation Function Estimates

B. Testing the US Assumption

In Section II-C, I noted that the US assumption is questionable for UWB channels. In order to test it, the only data available is the measured frequency response. However, since the measurements are only performed over a limited range of frequencies and with filters and averages introducing some measurement uncertainty, it is not clear a priori how the US assumption about the underlying continuous time channel can be assessed.

APPENDIX I COMMON DENSITIES

The following is a short summary of probability density functions and associated parameters for the common channel tap models and the distributions used in some of the tests. The formulas are compiled from the books by Papoulis [13], Proakis [14] and Weisstein [15].

A. Rayleigh

- PDF

$$f_X(x) = \frac{x}{\sigma^2} e^{-\frac{x^2}{2\sigma^2}} \quad (34)$$

- CDF

$$F_X(x) = 1 - e^{-\frac{x^2}{2\sigma^2}} \quad (35)$$

- domain $[0, \infty)$
- mean

$$\mathbb{E}[X] = \sqrt{\frac{\pi\sigma^2}{2}} \quad (36)$$

- variance

$$\text{Var}[X] = \left(2 - \frac{\pi}{2}\right)\sigma^2 \quad (37)$$

- higher moments

$$\mathbb{E}[X^k] = (2\sigma^2)^{\frac{k}{2}} \Gamma\left(1 + \frac{1}{2}k\right) \quad (38)$$

B. Rice

- PDF

$$f_X(x) = \frac{x}{\sigma^2} e^{-\frac{x^2+s^2}{2\sigma^2}} I_0\left(\frac{xs}{\sigma^2}\right) \quad (39)$$

with the modified Bessel function of the first kind I_0

- CDF

$$F_X(x) = 1 - Q_1\left(\frac{s}{\sigma}, \frac{x}{\sigma}\right) \quad (40)$$

with the Marcum Q-function

$$Q_1(a, b) = e^{-\frac{a^2+b^2}{2}} \sum_{k=0}^{\infty} \left(\frac{a}{b}\right)^k I_k(ab), \quad b > a > 0 \quad (41)$$

- domain $[0, \infty)$
- mean

$$\mathbb{E}[X] = \sigma \frac{\sqrt{\pi}}{2} \left(\left(1 + \frac{s^2}{2\sigma^2}\right) I_0\left(\frac{s}{2}\right) + s I_1\left(\frac{s}{2}\right) \right) e^{-\frac{s^2}{2}} \quad (42)$$

C. Nakagami

- PDF

$$f_X(x) = \frac{2}{\Gamma(m)} \left(\frac{m}{\Omega}\right)^m x^{2m-1} e^{-\frac{mx^2}{\Omega}} \quad (43)$$

- mean

$$\mathbb{E}[X] = \frac{\Gamma(m+1/2)}{\Gamma(m)} \sqrt{\frac{\Omega}{m}} \quad (44)$$

- variance

$$\text{Var}[X] = \Omega \left[1 - \frac{1}{m} \left(\frac{\Gamma(m+1/2)}{\Gamma(m)} \right)^2 \right] \quad (45)$$

- higher moments

$$\mathbb{E}[X^n] = \frac{\Gamma\left(m + \frac{1}{2}n\right)}{\Gamma(m)} \left(\frac{\Omega}{m}\right)^{\frac{n}{2}} \quad (46)$$

- domain $(0, \infty)$
- remarks: the parameters are defined as follows
 - $\Omega = \mathbb{E}[X^2]$
 -

$$m = \frac{\Omega^2}{\mathbb{E}[(X^2 - \Omega)^2]}, \quad m \geq \frac{1}{2} \quad (47)$$

m is called the *fading figure*

for $m = 1$, (43) reduces to the Rayleigh PDF (34).

D. Lognormal

- PDF

$$f_X(x) = \frac{1}{x\sqrt{2\pi\sigma^2}} e^{-\frac{(\ln(x)-\mu)^2}{2\sigma^2}} \quad (48)$$

- CDF

$$F_X(x) = \frac{1}{2} \left[1 + \text{erf}\left(\frac{\ln(x)-\mu}{\sqrt{2\sigma^2}}\right) \right] \quad (49)$$

- domain $(0, \infty)$
- mean

$$\mathbb{E}[X] = e^{\mu + \frac{\sigma^2}{2}} \quad (50)$$

- variance

$$\text{Var}[X] = e^{\sigma^2 + 2\mu} (e^{\sigma^2} - 1) \quad (51)$$

how to estimate the eigenvalues?

nonparametric estimates?

need correlation function estimate first; link to continuous channel correlation function

E. Central χ^2 with n Degrees of Freedom

The central χ^2 distribution arises as the distribution of the sum of n independent zero mean Gaussian random variables. If the variance is normalized to unity, the following expressions are obtained.

- PDF

$$f_X(x) = \frac{x^{\frac{n}{2}-1}}{2^{\frac{n}{2}}\Gamma(\frac{n}{2})} e^{-\frac{x}{2}} \quad (52)$$

- CDF

$$F_X(x) = 1 - \frac{\Gamma(\frac{1}{2}n, \frac{1}{2}x^2)}{\Gamma(\frac{1}{2}n)} \quad (53)$$

- domain $[0, \infty)$
- mean $\mathbb{E}[X] = n$
- variance $\text{Var}[X] = 2n$

A slightly different result is obtained for the sum of Gaussian random variables with variance σ^2 .

-

$$f_X(x) = \frac{x^{\frac{n}{2}-1}}{\sigma^n 2^{\frac{n}{2}}\Gamma(\frac{n}{2})} e^{-\frac{x}{2\sigma^2}} \quad (54)$$

- mean $\mathbb{E}[X] = n\sigma^2$
- variance $\text{Var}[X] = 2n\sigma^4$

F. Non-central χ^2

The non-central χ^2 distribution arises as the distribution of the the sum of n independent Gaussian

APPENDIX II HYPOTHESIS TESTING

The following is a short summary about hypothesis testing, extracted from the books by Papoulis [13], Bartoszyński [12] and Dixon [16]. Hypothesis testing is part of decision theory. The simplest case is the binary hypothesis testing problem, where some assumption, called the *null hypothesis* H_0 is tested against the *alternate hypothesis* H_1 . The null hypothesis might be for example the assumption that the distribution of a random variable X has parameter $\theta = \theta_0$. The alternate hypothesis would then be $\theta \neq \theta_0$. Hypothesis testing is not about determining whether H_0 or H_1 is true. It is to establish if the evidence in form of available data supports the hypothesis or not. Therefore the sample space is partitioned into the *critical region* \mathcal{D}_c and the *region of acceptance* \mathcal{D}_c^c . Depending on the location of the data points \mathbf{X} within the sample space, the hypothesis of the test is rejected or not. Some basic terminology in hypothesis testing is summarized as follows.

- If H_0 is true and $\mathbf{X} \in \mathcal{D}_c$, H_0 is rejected, called a *Type I error*. The probability

$$\alpha = \mathbb{P}(\mathbf{X} \in \mathcal{D}_c | H_0) \quad (55)$$

is called the *significance level* of the test.

- If H_0 is false and $\mathbf{X} \notin \mathcal{D}_c$, H_0 is accepted, called a *Type II error*. The probability of error is a function $\beta(\theta)$, called the *operating characteristic* (OC) of the test.

- The difference $P(\theta) := 1 - \beta(\theta)$ is the probability of rejecting H_0 when false, called the *power* of the test.

For so called “goodness-of-fit” tests, H_0 does not involve parameters. The hypothesis is, that a given function $F_0(x)$ equals the distribution $F(x)$ of a random variable X , $H_0 : F(x) \equiv F_0(x)$ against $H_1 : F(x) \neq F_0(x)$. These types of tests normally rely on some limiting behavior of a function of the data and the distribution under test, called the *test statistic*. The distribution of this test statistic converges to some other distribution if the data is indeed drawn according to the distribution under test. If not, then the test statistic will yield a value that would occur only with low probability according to the limiting distribution. This probability is set by the confidence level α of the test, and hence hypothesis where the test statistic exceeds the value of the CDF $Q(\alpha)$ need to be rejected.

A. The Kolmogorov-Smirnov Test

Let $F_i(x)$ be the empirical estimate of the CDF of the random variable X from the sample i and let $F_n(x)$ be the empirical CDF obtained from n independent samples. Then the distance

$$D_n := \sup_x |F_n(x) - F(x)| \quad (56)$$

converges to zero a.s. for $n \rightarrow \infty$. Hence for large n , D_n is close to zero if H_0 is true and close to $\sup_x |F_n(x) - F(x)|$ if $H - 1$ is true. The distribution of $\sqrt{n}D_n$ can be shown to converge to the Kolmogorov distribution

$$\lim_{n \rightarrow \infty} \mathbb{P}(\sqrt{n}D_n \leq z) = 1 - 2 \sum_{k=1}^{\infty} (-1)^{k-1} e^{-2k^2 z^2} =: Q(z). \quad (57)$$

The test should reject H_0 if the observed value of the statistic $\sqrt{n}D_n$ exceeds the critical value determined from the right tail of the distribution according to the significance level. $Q(z)$ is tabulated in any standard textbook, eg. [12, Table A7]. The test has power 1 against any alternative in the limit $n \rightarrow \infty$.

The test only applies if the distribution $F(x)$ of the null hypothesis is fixed. If the parameters need to be estimated from the samples, the corresponding distribution $F^*(x)$ is now *random*, depending on the same samples as the ones used to determine the empirical distribution F_n , and the limiting distribution of $\sqrt{n} \sup_x |F_n(x) - F^*(x)|$ is not given by $Q(z)$.

B. The χ^2 Test

1) *Discrete Distribution*: Let X be a discrete random variable defined on some finite alphabet \mathcal{X} with associated probabilities $p_i = \mathbb{P}(X = x_i)$. In a random sample of size N , each letter appears with frequency N_i , such that $\sum N_i = N$. The vector $[N_1, \dots, N_r]$ is called the *count vector*. The hypothesis to test is

$$H_0 : p_i = p_i^0, \quad i = 1, \dots, r \quad (58)$$

against the general alternative H_1 : H_0 is false. Here $\mathbf{p}^0 = [p_1^0, \dots, p_r^0]$ is some fixed distribution. The test statistic

$$Q^2 := \sum_{j=1}^r \frac{(N_j - np_j^0)^2}{np_j^0} \quad (59)$$

has the limiting distribution χ_{r-1}^2 , i.e. a central χ^2 distribution with $r - 1$ degrees of freedom, if the distribution of X equals the distribution of the null hypothesis. To obtain a good approximation, the counts should exceed 10. When there are many letters in the alphabet, the approximation is good enough even if few expected frequencies are as small as 1. The critical region of the test is the right tail of the χ^2 distribution with confidence level α , denoted $\chi_{\alpha, r-1}^2$ and tabulated in any standard statistics textbook [12, Table A4]. If now the test statistic exceeds this value, then the distribution of the sample can be only be drawn according to the distribution under test with low probability (with probability less than α to be precise). Hence this hypothesis has to be rejected.

2) *Continuous Distribution*: The above outlined test can be adapted to continuous distributions by partitioning the range of the random variable X , i.e. by creating r sets C_1, \dots, C_r that are disjoint and cover the whole range⁴. If $f(x)$ is the density of X specified by the null hypothesis, then

$$p_j^0 = \int_{C_j} f(x) dx, \quad j = 1, \dots, r. \quad (60)$$

The test now depends also on the choice of partition.

3) *Discrete Parametric Distribution*: Often the Distribution of the null hypothesis is not completely specified, such that just the family (e.g. Bernoulli, Poisson etc.) is known and the parameters are not. Denote the k -dimensional parameter vector by θ . Then the distribution of the discrete random variable X is given by $\mathbf{p}(\theta) = [p_1(\theta), \dots, p_r(\theta)]$ with $p_j(\theta) > 0$. Let the maximum likelihood estimate (MLE) of θ be denoted by $\hat{\theta}$. Then the statistic

$$Q^2 := \sum_{j=1}^r \frac{(N_j - np_j(\hat{\theta}))^2}{np_j(\hat{\theta})} \quad (61)$$

has the limiting χ^2 distribution with $r - 1 - k$ degrees of freedom as $n \rightarrow \infty$. Thus the test proceeds as before, but to compute the critical region, the distribution with the reduced number of degrees of freedom needs to be used.

4) *Continuous Parametric Distribution*: If the parametric distribution is continuous, the test methodology remains the same, i.e. the range of X needs to be partitioned and the respective probabilities are computed via the integral over the density function. However, the MLE of the parameter vector is now in general very hard to obtain. The key point is that $\hat{\theta}$ is no longer the the same for the continuous distribution and the discrete distribution obtained through partitioning. However, it is the latter MLE that is required to form the statistic (61). In most cases, $\hat{\theta}$ can only be obtained numerically. An example borrowed from Bartoszyński [12] illustrates this problem. Assume $X \sim \mathcal{N}(\mu, \sigma^2)$ and N_j is the count of observations in the interval $[t_{j-1}, t_j)$. The MLE is the solution to the system of equations

$$\frac{\partial \log L}{\partial \mu} = 0, \quad \frac{\partial \log L}{\partial (\sigma^2)} = 0 \quad (62)$$

with the likelihood function

$$L = \prod_{j=1}^r \left(\frac{1}{\sqrt{2\pi\sigma^2}} \int_{t_{j-1}}^{t_j} e^{-\frac{(x-\mu)^2}{2\sigma^2}} dx \right)^{N_j}. \quad (63)$$

If now the MLE from the complete data instead of the grouped data is used, the limiting distribution is unknown. However, there exists a bound. Let $\hat{\theta}^*$ be the MLE of the parameter vector based on the complete observation. Then the statistic

$$Q^{*2} := \sum_{j=1}^r \frac{(N_j - np_j(\hat{\theta}^*))^2}{np_j(\hat{\theta}^*)} \quad (64)$$

satisfies, as $n \rightarrow \infty$

$$\mathbb{P}(\chi_{r-1-k}^2 \geq t) \geq \lim_{n \rightarrow \infty} \mathbb{P}(Q^{*2} \geq t) \geq \mathbb{P}(\chi_{r-1}^2 \geq t) \quad (65)$$

for every $t \geq 0$. This implies that if the hypothesis can be rejected on the basis of the partitioned distribution with the unpartitioned parameter estimates, it will also be rejected if the partitioned parameter estimates are used.

REFERENCES

- [1] P. A. Bello, "Characterization of randomly time-variant linear channels," *IEEE Transactions on Communications*, vol. 11, pp. 360–393, 1963.
- [2] H. Artés, G. Matz, and F. Hlawatsch, "Linear time-varying channels," Department of Communications and Radio-Frequency Engineering, Vienna University of Technology, Vienna, Austria, Tech. Rep. 98-06, Dec. 1998.
- [3] J. Kunisch and J. Pamp, "Measurement results and modeling aspects for the UWB radio channel," in *IEEE Conference on Ultra Wideband Systems and Technologies Digest of Technical Papers*, 2002, pp. 19–23.
- [4] G. Matz, "Characterization of non-WSSUS fading dispersive channels," in *Proc. Int. Conference on Communications*, May 2003, pp. 2480–2484.
- [5] H. Hashemi, "The indoor radio propagation channel," *Proceedings of the IEEE*, vol. 81, no. 7, pp. 943–968, July 1993.
- [6] R. C. Qiu, "A study of the ultra-wideband wireless propagation channel and optimum UWB receiver design," *IEEE Journal on Selected Areas in Communications*, vol. 20, no. 9, pp. 1628–1637, Dec. 2002.
- [7] M. Hämäläinen, T. Pätsi, and V. Hovinen, "Ultra wideband indoor radio channel measurements," in *Proc. 2nd Finish Wireless Communications Workshop*, Tampere, Finland, Oct. 2001.
- [8] A. S. Y. Poon and M. Ho, "Indoor multiple-antenna channel characterization from 2 to 8 GHz," in *Proc. Int. Conference on Communications*, May 2003.
- [9] Á. Álvarez, G. Valera, M. Lobeira, R. Torres, and J. L. García, "Ultrawideband channel characterization and modeling," in *Proc. Int. Workshop on Ultra Wideband Systems*, Oulu, Finland, June 2003.
- [10] J. Keignart and N. Daniele, "Channel sounding and modelling for indoor UWB communications," in *Proc. Int. Workshop on Ultra Wideband Systems*, Oulu, Finland, June 2003.
- [11] P. Pagani, P. Pajusco, and S. Voinot, "A study of the ultra-wide band indoor channel: Propagation experiment and measurement results," in *Proc. Int. Workshop on Ultra Wideband Systems*, Oulu, Finland, June 2003.
- [12] R. Bartoszyński and M. Niewiadomska-Bugaj, *Probability and Statistical Inference*. New York, NY, USA: Wiley, 1996.
- [13] A. Papoulis and S. U. Pillai, *Probability, Random Variables and Stochastic Processes*, 4th ed. Boston, MA, USA: McGraw-Hill, 2002.
- [14] J. G. Proakis, *Digital Communications*, 4th ed. New York, NY, USA: McGraw-Hill, 2001.
- [15] E. W. Weisstein, "Eric weisstein's world of mathematics," site visited Apr. 2004. [Online]. Available: <http://mathworld.wolfram.com>
- [16] W. J. Dixon and F. J. Massey, Jr., *Introduction to Statistical Analysis*, 4th ed. New York, NY, USA: McGraw-Hill, 1983.

⁴The sets need not necessarily be intervals.

S-V Parameter Extraction: General Guidelines

Chia-Chin Chong, *Member, IEEE*

Abstract—This document gives some general guidelines on the procedures to extract Saleh-Valenzuela (S-V) channel parameters from measurement data.

I. INTRODUCTION

THE aim of this document is to give some general guidelines on the procedures to extract Saleh-Valenzuela (S-V) channel parameters from measurement data.

II. S-V MODEL REVISITED

The Saleh-Valenzuela (S-V) model [1] is based on the clustering of multipath components (MPCs) observed in the measurement data. The discrete-time impulse response is given by

$$h_{discr}(t) = \sum_{l=0}^L \sum_{k=0}^{K_l} a_{k,l} \delta(t - T_l - \tau_{k,l}), \quad (1)$$

where $\delta(\cdot)$ is the Dirac delta function, L is the number of clusters and K_l is the number of MPCs within the l^{th} cluster, $a_{k,l}$ is the tap weight (or multipath gain coefficient) of the k^{th} component in the l^{th} cluster, T_l is the delay of the l^{th} cluster which is defined as the time-of-arrival (TOA) of the first arriving MPC within the l^{th} cluster and $\tau_{k,l}$ is the delay of the k^{th} MPC relative to the l^{th} cluster arrival time, T_l . By definition, we have $\tau_{0,l} = 0$. The distributions of the cluster arrival times (or inter-arrival times), T_l and the ray arrival times (or intra-arrival times), $\tau_{k,l}$ are given by two Poisson processes. Thus, according to this model, T_l and $\tau_{k,l}$ are described by the independent interarrival exponential probability density functions (pdfs) as follows

$$p(T_l | T_{l-1}) = \Lambda \exp[-\Lambda(T_l - T_{l-1})], \quad l > 0 \quad (2)$$

$$p(\tau_{k,l} | \tau_{(k-1),l}) = \lambda \exp[-\lambda(\tau_{k,l} - \tau_{(k-1),l})], \quad k > 0 \quad (3)$$

where Λ is the cluster arrival rate, and λ is the ray arrival rate. Typically, each cluster consists of many rays where $\lambda \gg \Lambda$.

Chia-Chin Chong is with the RF Technology Group, i-Networking Lab., Samsung Advanced Institute of Technology (SAIT), Suwon, Korea. E-mail: chiachin.chong@samsung.com.

The average power of both the clusters and the rays within the clusters are assumed to decay exponentially, such that the average power of a MPC at a given delay, $T_k + \tau_{k,l}$ is given by

$$\overline{a_{k,l}^2} = \overline{a_{0,0}^2} \cdot e^{-T_l/\Gamma} \cdot e^{-\tau_{k,l}/\gamma} \quad (4)$$

where $\overline{a_{0,0}^2}$ is the expected value of the power of the first arriving MPC, Γ is the decay exponent of the clusters and γ is the decay exponent of the rays within a cluster. Typically, $\Gamma > \gamma$ and the expected power of the rays in a cluster decay faster than the expected power of the first ray of the next cluster.

Here, lognormal distribution rather than Rayleigh distribution for the multipath gain magnitude is adopted as described in [13] and [14]. [13] suggests two independent lognormal variables to represent the amplitude variations of the clusters and rays. However, these random variables can be combined as a single lognormal random variable. The polarity of the path is represented as an equiprobable binary random variable, $p_{k,l}$ taking on the values $+/-1$ to account for signal inversion due to reflections. Thus, the multipath gain coefficient is given by

$$\begin{aligned} a_{k,l} &= p_{k,l} \xi_l \beta_{k,l} \\ &= p_{k,l} 10^{(\mu_{k,l} + X_{\sigma,k,l})/20} \end{aligned} \quad (5)$$

where ξ_l reflects the fading associated with l^{th} cluster, and $\beta_{k,l}$ corresponds to the fading associated with the k^{th} ray of the l^{th} cluster given by

$$|\xi_l \beta_{k,l}| = 10^{(\mu_{k,l} + X_{\sigma,k,l})/20}, \quad (6)$$

while $\mu_{k,l}$ and $X_{\sigma,k,l}$ are given by

$$\mu_{k,l} = \frac{20 \ln(|\overline{a_{0,0}^2}|) - 10T_l/\Gamma - 10\tau_{k,l}/\gamma}{\ln(10)} - \frac{\sigma^2 \ln(10)}{20}, \quad (7)$$

$$X_{\sigma,k,l} = N(0, \sigma^2), \quad (8)$$

where σ is in dB.

Fig. 1 and Fig. 2 illustrate the S-V model channel impulse

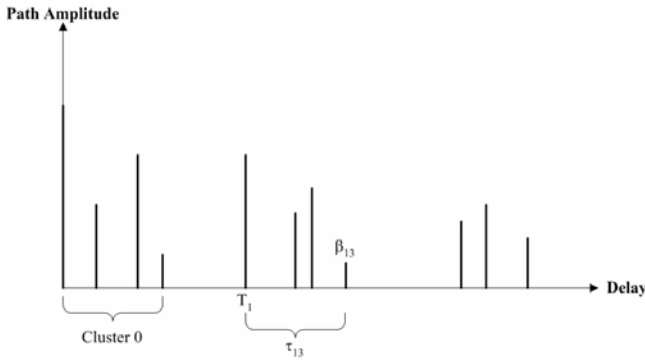


Fig. 1. An illustration of channel impulse response [15].

responses (CIRs) and double exponential decay model, respectively.

III. CHANNEL MEASUREMENT TECHNIQUES

Generally, there are two techniques to perform channel measurements. Firstly, is the time-domain technique in which measurement usually performed using digital sampling oscilloscope (DSO). UWB measurements conducted using this method was reported in [2]–[6]. This technique measured the channel impulse response (CIR), $h(t)$. Secondly, is the frequency-domain technique in which measurement usually performed using vector network analyzer (VNA). UWB measurements conducted using this technique was reported in [6]–[12]. This technique measured the channel transfer function (CTF), $H(f)$. A more detail list of literature overview of UWB channel soundings and models is reported in [18].

IV. DATA ANALYSIS AND PARAMETERS EXTRACTION

A. Data Post-Processing

Since the measurement system measured the “radio channel” (i.e. including the effect of amplifiers, cables and antennas), in order to remove these hardware effects, all raw data are normalized with the calibration data so that only the “propagation channel” data will be used for further analysis. For measurements conducted using VNA, the CTFs are transformed into the CIRs through inverse Fourier transform (IFT). Frequency domain windowing is applied prior to the transformation to reduce the leakage problem. Then, the CIRs are analyzed by divided the temporal axis into small intervals (or delay bins), $\Delta\tau$. This delay bin is corresponding to the width of a path and is determined by the reciprocal of the bandwidth swept (i.e. time resolution of the measurement system). The CIRs are then normalized such that the total power in each power delay profile (PDP), $P(\tau)$ is equal to one. A cutoff threshold of 20 dB below the strongest path was applied to the PDP so that any paths arrived below his threshold is set to zero. This is to ensure that only the effective paths are used for the channel modeling. The initial delay for each of the transmission links was extracted from the PDP. This value was removed from the results so that all PDPs can be aligned with

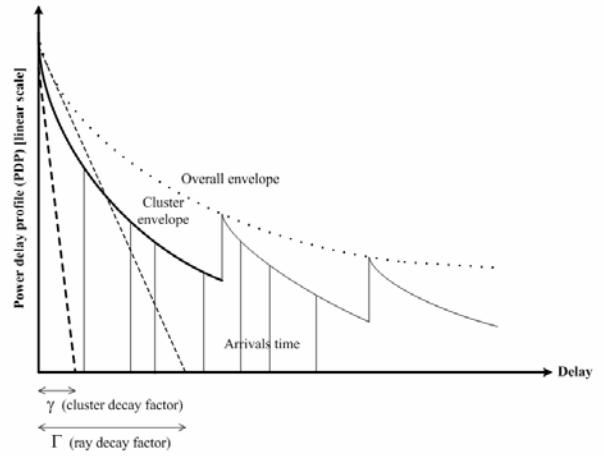


Fig. 2. An illustration of exponential decay of mean cluster power and ray power within clusters [17].

first path arrives at 0 ns.

B. Cluster Identification

The first task is to identify clusters. Different researchers have different definitions of a cluster. The position and the size of the clusters will be heavily dependent on the superstructure and physical layout of the considered environments. However, clustering identification employing statistical techniques such as clustering algorithms are inappropriate for this application as it is very difficult to develop a robust algorithm for the automatic identification of cluster regions. Thus, cluster regions were selected manually by visual inspection. Both [1] and [16] also deploy visual inspection to identify clusters from their measurement data.

C. Arrival Statistics

In order to analyze the statistics of the clustering effects, the clusters in each data set must be identified. With the times and amplitudes of all major arrivals identified, as well as their clustering patterns, the data could be used to analyze the statistics and arrive at a model. As shown in Section II, there are 5 key parameters that define the S-V model:

- Λ is the cluster arrival rate
- λ is the ray arrival rate, i.e. the arrival rate of path within each cluster
- Γ is the cluster exponential decay factor
- γ is the ray exponential decay factor
- σ is the standard deviation of the lognormal fading term (dB)

Note that we have assumed that all the above parameters are the same for all clusters. Following [13], the above parameters are found using “brute force search” by trying to fit the measurement data to match different important characteristics of the channel. The main characteristics of the channel that are used to derive the above model parameters are the following:

- Mean excess delay, τ_m
- rms delay spread, τ_{rms}
- Number of MPCs within 20 dB threshold, NP_{20dB} .

The *mean excess delay*, τ_m is the first moment of the PDP [19]

$$\tau_m = \frac{\sum_k a_k^2 \tau_k}{\sum_k a_k^2} = \frac{\sum_k P(\tau_k) \tau_k}{\sum_k P(\tau_k)}, \quad (9)$$

and the *rms delay spread*, τ_{rms} is the square root of the second central moment of the PDP [19]

$$\tau_{rms} = \sqrt{\tau_m^2 - (\tau_m)^2}, \quad (10)$$

where

$$\tau_m^2 = \frac{\sum_k a_k^2 \tau_k^2}{\sum_k a_k^2} = \frac{\sum_k P(\tau_k) \tau_k^2}{\sum_k P(\tau_k)}. \quad (11)$$

The number of MPCs for each of the PDP was found by counting all MPCs that are within 20 dB of the strongest path. Note that, the binned data were used here.

Following the methodology in [16], firstly, the cluster and ray decay time constants, Γ and γ , were estimated by superimposing clusters with normalized amplitudes and time delays and selecting a mean decay rate. For example, in order to estimate Γ , the first cluster arrival in each set was normalized to an amplitude of one and a time delay of zero. All cluster arrivals were superimposed and plotted on a semi-logarithmic plot. The estimate for Γ was found by curve fitting the line (representing an exponential curve) such that the mean squared error was minimized. Similarly, in order to estimate γ , the first arrival in each cluster was set to a time of zero and amplitude of one, and all other ray arrivals were then adjusted accordingly and superimposed. Following this model, the best fit exponential distributions were determined from the cluster and ray arrival times, respectively. In order to estimate the Poisson cluster arrival rate, Λ the first arrival in each cluster was considered to be the beginning of the cluster, regardless of whether or not it had the largest amplitude. The arrival time of each cluster was subtracted from its successor, so that the conditional probability distribution given in (2) could be estimated. The Poisson ray arrival rate, λ was guessed based on the average separation time between arrivals. Estimates for Λ and λ were both done by fitting the sample pdf to the corresponding probability for each bin. The fitting was done using a least mean square criterion.

For the case of overlapping clusters, procedure as proposed in [21] is adopted. By assuming that each cluster has an exponential shape, a straight-line extrapolation function (in dB) is deployed on the first cluster and then subtract the PDP of the first cluster from the total PDP. Then, the next non-overlapping region is used to extract the decay factor for the next cluster.

This process is repeated for all clusters in the total PDP until the last cluster is reached. Note that the powers of overlapping rays are calculated so that the total sum of the powers of overlapping rays corresponding to different clusters equals to the powers of the original total PDP. More details of this procedure is reported in [21].

D. Amplitude Statistics

It is important to evaluate the probability distribution of the random amplitudes while fitting the empirical data to a channel model. For example, the original S-V model assumed that the path amplitudes had a Rayleigh distribution. However for the case of UWB base band pulses, this cannot necessarily be assumed. In order to get an idea of how the individual paths are distributed at different delays across the entire measurement set, similar approaches as in [20] is adopted by comparing the fittings of empirical distributions of path amplitudes obtained from measurement data to theoretical distributions. The following procedure can be summarized as follows:

- The received data was binned so that the amplitude of each bin would signify the amplitude of the multipath component in that bin.
- Data from bins at specific delays from the entire measurement set were matched to theoretical distributions such as Rayleigh, Lognormal, Ricean, Nakagami, Gamma, etc.
- Elaborate the goodness-of-fit tests (e.g. Kolmogorov-Smirnov test and/or Chi-Square test) to find the best fit among all the theoretical distributions.

It was observed in [15] that the log-normal distribution gives the best match to the obtained data. The log-normal cumulative distribution function (cdf) can be written as

$$F(x | \mu, \sigma) = \frac{1}{\sigma\sqrt{2\pi}} \int_0^x \frac{e^{-\frac{(\ln(t)-\mu)^2}{2\sigma^2}}}{t} dt. \quad (12)$$

This is equivalent to the normal distribution when the amplitudes and the statistics are expressed in log scale $20 \log_{10}(A)$. The received signal amplitudes are expressed in dB and the mean, μ and the standard deviation, σ are calculated using the dB values.

V. CONCLUSION

General guidelines on the procedures to extract S-V channel parameters from the measurement data have been described. These parameters including cluster and ray arrival rates, cluster and ray exponential decay factors and the standard deviation of the lognormal fading term.

REFERENCES

- [1] A. A. M. Saleh and R. A. Valenzuela, "A statistical model for indoor multipath propagation," *IEEE J. Select. Areas Commun.*, vol. 5, no. 2, pp. 128-137, Feb. 1987.

- [2] M. Z. Win and R. A. Scholtz, "Characterization of ultra-wide bandwidth wireless indoor channels: a communication-theoretic view," *IEEE J. Select. Areas Commun.*, vol. 20, no. 9, pp. 1613-1627, Dec. 2002.
- [3] D. Cassioli, M. Z. Win and A. F. Molisch, "The ultra-wide bandwidth indoor channel: from statistical model to simulations," *IEEE J. Select. Areas Commun.*, vol. 20, no. 6, pp. 1247-1257, Aug. 2002.
- [4] R. J. -M. Cramer, R. A. Scholtz and M. Z. Win, "Evaluation of an ultra-wide band propagation channel," *IEEE Antennas and Propagation*, vol. 50, no. 5, pp. 561-569, May. 2002.
- [5] M. Pendergrass and W. C. Beeler, "Empirically based statistical UWB channel model," IEEE P802.15-02/240SG3a, Jul. 2002.
- [6] L. Rusch, C. Prettie, D. Cheung, Q. Li and M. Ho, "Characterization of UWB propagation from 2 to 8 GHz in a residential environment," submitted to *IEEE J. Select. Areas Commun.*
- [7] J. Keignart and N. Daniele, "UWB channel modeling contribution from CEA-LETI and STMicroelectronics," IEEE P802.15-02/444, Nov. 2002.
- [8] A. Alvarez, G. Valera, M. Lobeira, R. F. Torres and J. L. Garcia, "UWB channel model contribution from University of Cantabria and ACORDE," IEEE P802.15-02/445r1, Nov. 2002.
- [9] V. Hovinen, M. Hamalainen, R. Tesi, L. Hentila and N. Laine, "A proposal for an indoor UWB path loss model," IEEE P802.15-02/280, Jul. 2002.
- [10] J. Kurnisch and J Pamp, "Radio channel model for indoor UWB WPAN environments," IEEE P802.15-02/318, Jul. 2002.
- [11] S. S. Ghassemzadeh, R. Jana, C. Rice, W. Turin and V. Tarokh, "Measurement and modeling of an ultra-wide bandwidth indoor channel," *IEEE Trans. Commun.*, in press.
- [12] P. Pagani, P. Pajusco and S. Voinot, "A study of the ultra-wide band indoor channel: propagation experiment and measurement results," COST 273 TD(03)060, Jan. 2003.
- [13] J. Foerster, "Channel Modeling Sub-committee Report (Final)," IEEE P802.15-02/490r1-SG3a, Feb. 2003.
- [14] A. F. Molisch, "Status of models for UWB propagation channels," IEEE P802.15-04/195r0, Mar. 2004.
- [15] J. Foerster, "UWB channel modeling contribution from Intel," IEEE P802.15-02/279r0-SG3a, Jun. 2002.
- [16] Q. H. Spencer, B. D. Jeffs, M. A. Jensen and A. L. Swindlehurst, "Modeling the statistical time and angle of arrival characteristics of an indoor multipath channel," *IEEE J. Select. Areas Commun.*, vol. 18, no. 3, pp. 347-359, Mar. 2000.
- [17] J. Keignart and N. Daniele, "Channel sounding and modeling for indoor UWB communications," *International Workshop on Ultra Wide Band Systems 2003*.
- [18] U. Schuster, "UWB channel soundings and models – literature overview," IEEE P802.15-04/196r0.
- [19] T. S. Rappaport, *Wireless Communications: Principles and Practice*, Prentice Hall PTR, Upper Saddle River, NJ, USA, 2nd edition, 2002.
- [20] H. Hashemi, "Impulse response modeling of indoor radio propagation channels," *IEEE J. Select. Areas Commun.*, vol. 11, no. 7, pp. 967-977, Sep. 1993.
- [21] V. Erceg *et. al.*, "TGn channel models," IEEE P802.11-03/940r2, Jan. 2004.